ADVANCED MATERIALS TECHNOLOGIES
www.advmattechnol.de

Performance Study of Graphene Oxide as an Antierosion Coating for Ornamental and Heritage Dolostone

Rebeca Martínez-García, David González-Campelo, Fernando J. Fraile-Fernández, Ana María Castañón, Pablo Caldevilla, Sara Giganto, Almudena Ortiz-Marqués, Flavia Zelli, Víctor Calvo, José M. González-Domínguez, and María Fernández-Raga**

Concern for the perpetuation of stone monuments is deeply ingrained in humans; however, despite the attempts made in this field, there is still a great deal of effort needed to bring about advancements in the conservation of ornamental stone. Erosive agents, such as rain, extreme temperatures, and chemical and biological agents, threaten our stone heritage and gradually wear away buildings, sculptures, and other monuments found all around the world. Limestone and dolostone have been widely used throughout history, given their ease of extraction and workability. Nevertheless, these properties make them particularly vulnerable to the aforementioned erosive agents, for which the main solution at present is costly and time-consuming restoration. Given the scarcity of effective and durable agents to prevent the deterioration of ornamental and heritage stones, and as graphene oxide (GO) has recently shown impressive effectiveness for this task, this work will further explore the viability of GO as a protective coating for monumental dolostone. For this purpose, GO is sprayed over dolostone surfaces by water dispersion with no adjuvants. The coating performance is assessed in terms of thermal stress, optical inspection (structured light 3D scanner), colorimetry, leachate analysis, and electron microscopy. The main results show that spray-coated GO over stone surfaces creates a highly protective and durable barrier without altering their aesthetic qualities.

1. Introduction

The notion of cultural heritage was first conceived and the term "historical monument" coined in the late 18th century, and since the emergence of this new mindset in favor of preserving historical heritage, countless resources have been invested for this purpose.[1] The current concept of an asset of cultural interest (ACI), which is codified at a legislative level in the Spanish Historical Heritage Law,[2] defines an ACI as a historical-artistic fact, a manmade material product, and an expression of a specific culture and society that has value as a material witness and resource. This definition delineates and identifies, albeit very briefly, the distinctive elements of any ACI. Because it qualifies as both a monument and a document, its value is intrinsic to its materiality and must therefore be protected. The dual connotation of heritage and resource requires physical safeguarding to ensure its permanence over

R. Martínez-García, F. J. Fraile-Fernández, A. M. Castañón, P. Caldevilla, A. Ortiz-Marqués
Department of Mining Technology
Topography and Structures
University of León
Campus de Vegazana s/n, León 24071, Spain

D. González-Campelo, M. Fernández-Raga
Department of Applied Physics
University of León
Campus de Vegazana s/n, León 24071, Spain
E-mail: maria.raga@unileon.es

S. Giganto
Area of Manufacturing Engineering
Universidad de León
Campus de Vegazana, León 24071, Spain

F. Zelli
Theory of Architecture and Architectural Projects
University of Valladolid
ETSAVA Avda. Salamanca 18, Valladolid 47014, Spain

V. Calvo, J. M. González-Domínguez
Group of Carbon Nanostructures and Nanotechnology (G-CNN)
Instituto de Carboquímica (ICB-CSIC)
C/ Miguel Luesma Castán 4, Zaragoza 50018, Spain
E-mail: jmgonzalez@icb.csic.es

The ORCID identification number(s) for the author(s) of this article can be found under https://doi.org/10.1002/admt.202300486

DOI: 10.1002/admt.202300486

time and its transmission with historical consistency to new generations.[3] Where historical heritage-based structures are concerned, limestone and dolostone have been used as the construction material for a very large number of monuments.

Dolostone or dolomite is a sedimentary crystalline type of $CaMg(CO_3)_2$ that is formed by an ion exchange substitution of calcium for magnesium in limestone ($CaCO_3$), resulting in many stones comprising a mixture of the minerals calcite and dolomite. Their ease of quarrying and workability have allowed dolostones to be shaped for the construction of countless monuments, sculptures, and other elements that have been included in the list of World Heritage sites. These constructions are usually found outdoors, thus subjected to climatic weathering. Dolostone has been cut into ashlars and paving slabs, used as a raw material for quicklime, and as part of the composition of asphalts and concretes. Consequently, structures built from limestone, dolostone, and other carbonated stones are present all over the world, outstanding examples of which are the Colosseum, the Notre-Dame Cathedral, the Great Pyramid of Giza, and the Taj Mahal.[4] Limestone and dolostone naturally show excellent resistance to compression; therefore, most extant historical buildings and sculptures are still standing in relatively good condition. However, water from streams and rainfall is very erosive, particularly in acidic conditions. CO_2 in the environment, whose concentration has been rising rapidly in recent decades,[5] accelerates the weathering of stones when combined with water.[6] Hence, dolostone is destined to undergo a process of deterioration that will devastate the legacy left by our ancestors,[7] and human action is essential if this situation is to be reversed.[8–11]

The three most significant phenomena leading to dolostone weathering are rainfall, high diurnal temperature variation, and, indirectly, nitrate and CO_2 pollution. Rainfall is the main phenomenon,[12,13] causing chemical dissolution that is accelerated by the intrinsic porosity of dolostone. The impact strength of precipitation in the form of raindrops and hailstones is also crucial. The combination of water with impurities leads to the form of degradation known as stone decay, which occurs when the stone surface crumbles into dust and grit.[14] Consequently, the outermost parts become detached, thus exposing the interior of the stones to the erosive agents. Unless there is an overall reduction in our carbon footprint, and transport and heating systems become less polluting,[15] combustion gases such as NO_x and CO_2 will continue to have a constant and very negative effect on dolostone and limestone. Moreover, high diurnal temperature variations, notably those taking place drastically and/or involving subzero temperatures produce internal tensions. This happens mostly through gelifraction, when these temperature variations are combined with frequent rainfall or high relative humidity, allowing water to percolate through the stones and, after freezing, cause fracturing that facilitates further water infiltration.[16] It is also important to mention the drastic changes that can be caused by variations in rainfall and temperature to the biotic communities found on sandstone and limestone heritage structures, which may switch from biodeteriogenic to bioprotective or vice versa.[17]

Parallel to the theoretical evolution of the notion of heritage, the need to preserve our tangible heritage, particularly that comprising stone-based structures, has given rise to the conceptual framework of the heritage landscape. This also entails an evolution in professional practice, fueling debate regarding the diversity and often conflicting attitudes to the criteria and principles of restoration. Protecting the stones that make up our oldest historical heritage (limestone and dolostone) from the damage caused by aggressive climate-induced processes is of global concern, requiring solutions to maintain their cultural and functional values.[11,14] Conservation is currently considered the priority alternative to restoration, with both actions being part of a common intervention aimed at understanding, safeguarding, protecting, and enhancing the value of our historical and cultural heritage, as specified by UNESCO since 1996.[18] Conservation implies the use of any technical operations suitable for conserving the material consistency of a heritage asset and reducing the extrinsic factors of degradation before returning it to society for its use and enjoyment. This corresponds with the most widely agreed principles at present: durability, reversibility, compatibility, and sustainability. Within this complex scenario, the modern science of conservation represents an important area of research, covering both the analytical characterization of ancient materials and the chemical reactions involved in their pathologies, and the search for new scientific methods for their preservation. Indeed, many and varied advances have seen the light in the last three decades related to the development of sustainable procedures for the production of nanoscale metal oxide/hydroxide particles, the synthesis of which opens up new perspectives for the protection and conservation of the cultural heritage of historical and architectural importance.[19] Nanotechnology provides innovative methods for a long-lasting and compatible preservation of monuments that are currently being used in a diffuse way for their consolidation, cleaning, deacidification, and preventive monitoring, and they are widely used in restoration works the world over.[20,21] As far as limestones and dolomites are concerned, nanoparticles are used mainly for their consolidation and surface cleaning (in the form of microemulsions), commonly consisting of $Ca(OH)_2$, $Mg(OH)_2$, and $Ba(OH)_2$.

Currently, restoration processes are laborious, costly, and only considered a short-term solution as they do not effectively stop the degradation of monuments. Furthermore, not all monuments are compatible with the available techniques, given the alterations that they cause to the stones. The application of conventional protective coatings to stone monuments exposed to weathering is increasingly being discouraged as these would affect their original aesthetics, a crucial feature for maintaining their value. Likewise, any coating designed for this purpose should involve convenient preparation and application procedures, plus affordability and the ability to be prepared in large quantities if the intention is to extend its use to large stone monuments. Thus, there is a demand to find new innocuous, functional, undetectable, long-lasting, and inexpensive treatments. And it is in this context that graphene derivatives emerge as a possible solution.[22] Even where pristine graphene is not generally accessible, other materials in the graphene family retain some of its special properties and, as in the case of the graphene oxide (GO), possess new ones (hydrophilicity, chemical versatility, etc.), while being much more affordable. Furthermore, the application of GO to other materials is effortless because the preparation process only involves dispersion in water.[23,24] In an earlier work, we demonstrated the efficient protective effects of GO on ornamental dolomite stones by the simple surface application of an additive-free aqueous colloid as a spray without significantly

altering their original aspect.[25] Such a GO coating can effectively stop the deterioration of the historical (carbonated stones) and industrial (cement and concrete) heritage structures, in terms of water-induced degradation, extending its use to both present and future architectures.[26,27]

The research results presented here further demonstrate the excellent effectiveness of the GO coating as a protective nanoscale barrier to shield stone monuments in the context of simulated conditions of strong rainfall and drastic temperature variations. The proposed spraying method has been proven to prevent physical damage to heritage stones caused by climatic weathering. Furthermore, this method is easy to apply as it relies in an additive-free, aqueous colloidal suspension of GO that can be directly sprayed onto the stones. As a result of its application, robust protection is achieved without altering the physical appearance of the monument in terms of either gloss or color when the appropriate concentration and methodology is utilized for each surface.[25]

The novelty of this work lies in the assessment of durability conditions provided by the GO coating on monumental dolostone whose aim is to minimize the impact of damage caused by climatic erosion. To the best of our knowledge, no other study has devoted such extensive analysis to the performance of any coating, GO in particular, on carbonated stones in terms of coating endurance, extent of erosion caused by simulated weather conditions, and evaluation of any impact on stone color and resistance.

2. Experimental Section

2.1. Previous Considerations

The research presented in this work is particularly focused on providing a strong basis for the preservation of monuments made of dolostone in western Europe in general, and more specifically in the province of León, northwestern Spain. The climate of this province climate was notably harsh due to its prominent continental character, and it presented huge differences commensurate with its varied and complex topography. Average temperatures and precipitation varied greatly between the lower-lying plains (>+10 °C, <400 mm, <75 days with precipitation) and the mountainous regions (<+5 °C, >1200 mm, >100 days with precipitation). There were ≈75 days of below-freezing temperatures per year on the plains, whereas this number rose to more than 100 in the mountains. The temperature often fell to −5 °C throughout the entire province, with low-lying areas experiencing temperatures above +35 °C on certain days.[28,29] These contrasts directly jeopardized the preservation of dolostone, justifying their need for protection.

Limestone and dolostone are present in numerous monuments around the world, and they are prevalent in northern Spain and in many parts of Europe. Both limestone and dolomite are sedimentary rocks, and their compressive strength is greater when stones are placed in the same position in which the sediment deposits were accumulated. Limestone largely comprises the mineral calcite, which has a composition relatively close to pure $CaCO_3$, with 54% CaO and 44% CO_2, and it occurs in sedimentary layers where calcite is the predominant mineral. Dolomite largely comprises the mineral dolomite, which is a double carbonate of Ca and Mg, $CaMg(CO_3)_2$ in which the Ca:Mg ratio varies between 58:42 and 47.5:52.5. It is formed by the action of Mg-rich water on calcareous deposits, where calcium is gradually replaced by magnesium. The extreme form of $MgCO_3$ is magnesite (MgO 47.8% and CO_2 52.2%), a scarce mineral that generally appears in seams derived from the alteration of igneous and metamorphic rocks.[30,31] In order to disambiguate between the two uses of dolomite, mineral and rock, the latter is referred to in this work by the term dolostone. Particular reference is made to Spanish Boñar dolostone, a crystalline rock that is fine-grained (less than 20 microns), consistent, almost completely dolomitized, compact, and idiomorphic. Its pores are filled with 15% spathic crystals with much larger unit sizes of up to 200 microns. It has a golden color, sometimes with reddish tones due to the sporadic presence of iron oxides, and with some quartz, calcite, and clay inclusions, which make it especially vulnerable to natural erosive agents, such as water and high diurnal temperature variation.[32,33]

2.2. Materials

The dolostone samples were directly extracted from their native quarry in Boñar, Spain, located at (42.857086, −5.315570). The samples were prepared by cutting into regular 50-mm cubes (135 in total), according to UNE 1926:2007[34] and 15801:2010[35] standards, among others. The GO used in this experiment was self-prepared by a preliminary synthesis of GO that involved applying the well-known Hummers oxidation method[36] to graphite flakes. The improvement proposed by Marcano et al.[37] was also applied, consisting of the addition of H_3PO_4 (10%) to the reaction medium to give rise to a material with a higher degree of oxidation and a more regular and less altered basal plane structure. The GO was finally obtained after ultrasonic exfoliation in water. The detailed preparation method can be found elsewhere,[25] together with a full characterization.

2.3. Methods

The coating of the dolostone samples was performed by simple airbrush spraying of an additive-free GO aqueous suspension (at 0.5 mg mL^{-1}), the procedure for which is reported elsewhere.[25] According to those previous results, in which every sprayed coat had a GO surface concentration of 3.3 μg cm^{-2}, and given that the best protection efficiency (with minimum variation in color) was demonstrated for 6.6 and 9.9 μg cm^{-2} GO, respectively, so this work focused on such GO surface concentrations.

A series of artificial rainfall simulation and temperature variation tests were designed for application to both protected and unprotected stones in order to gauge their erosive impact. **Figure 1** summarizes the experimental methodology used in this study, as well as the workflow followed throughout the research to assess the effectiveness of the GO coatings on the dolostone samples after erosion experiments.

The structure of the tests shown in this work were organized into three main parts, in sequential order:

1) A set of erosion tests, where dolostone samples were subjected to artificial rainfall via a rainfall simulator. This was

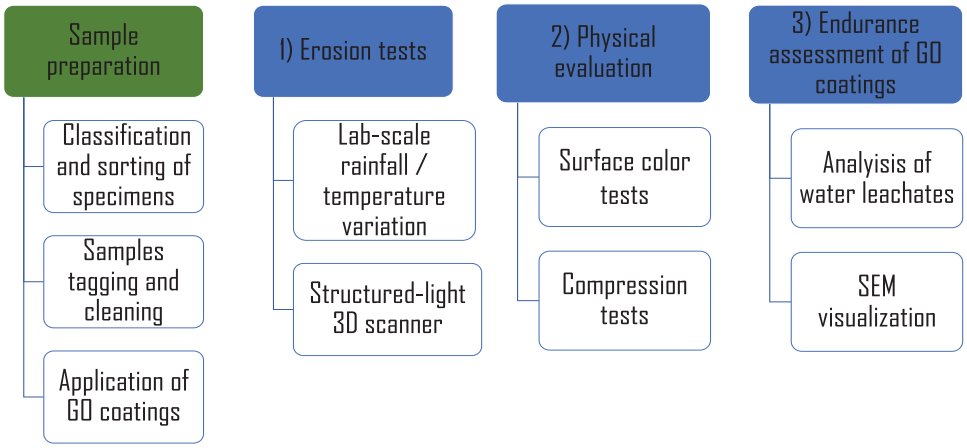

Figure 1. Schematic representing the methodology for evaluating the protective capabilities of GO coatings on dolostone samples.

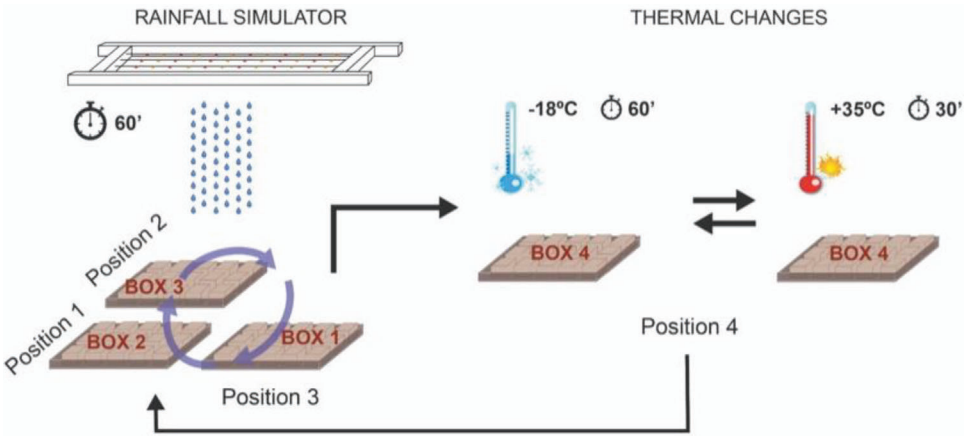

Figure 2. Scheme of the steps carried out at a laboratory scale of rainfall and temperature variation simulation.

carried out to replicate the most aggressive rainfall conditions experienced by the city of León, Spain, as well as the extreme diurnal temperature variations common to this area.[29,38] The erosion outcome was assessed by means of a structured-light 3D scanner in order to accurately ascertain the extent of wear on the samples.

2) A set of tests for the purpose of analyzing how the physical properties of the stones could have changed by the addition of the coating and/or the occurrence of climate simulations. These were conducted by examining changes in surface color and compressive strength.
3) Another set of tests were performed to analyze the durability, resistance, and stability of the GO-dolomite interfacial affinity in order to rule out possible detaching phenomena that could pose environmental hazards; they were also intended to ensure the approximate durability of the coating. This was done by examining the water leachates using different techniques, including inductively coupled plasma with optical emission spectroscopy (ICP-OES) and examining the dolostone surfaces by scanning electron microscopy (SEM).

2.3.1. Simulated Erosion Tests

Sample specimens were subjected to two types of environmental stress tests during a period of one year: wear, through the application of artificial rain, and the artificial variation of temperatures. These were intended to accelerate natural erosion by simulating the main natural erosive agents that affect dolostones. The erosion tests consisted of rainfall simulations (1 hour's rainfall in a 1-min interval, with 5-second pauses between intervals) and temperature variations (1 h at a temperature of −18 °C, followed by 30 min at a temperature of 35 °C) in repeated cycles as shown in **Figure 2**. The specimens were placed inside separate boxes underneath the rainfall simulator. Every day, a different box with different samples was removed and taken to the heat exchange chamber, leaving the remaining samples under the influence of the rainfall simulator. Three complete temperature cycles were carried out daily inside this chamber. The following day, this box was replaced by the subsequent one in the working field, so that eventually all the specimens underwent the same number of temperature cycles and equal exposure to rainfall times and

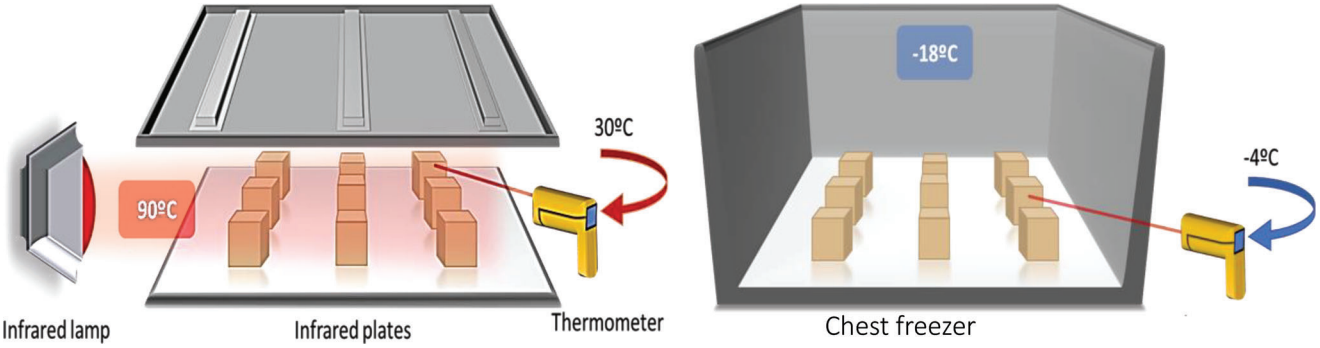

Figure 3. Visual depiction of the heating (left) and cooling (right) procedures applied to stone samples.

intensities (Figure 2). Photographs of the actual working setup are shown in Figure S1, Supporting Information.

Rainwater Considerations: The composition of rain varies depending on the city, its origin, and the main industrial or non-industrial activities that the rain encounters before landing on surfaces. Because of this, it was of interest to ascertain the actual composition of the proximate rainfall. Therefore, characterization was made of a large volume of natural rain (collected in the city of León in January, 2020) that would allow comparison to be made with the characteristics of the water actually used, which mainly consisted of deionized water. To be more precise, after some initial tests carried out with deionized water, the entire set of experiments were carried out with deionized water supplemented with natural rainwater collected in the vicinity of the work space, with a view to increase the available water for the tests. By saving and recirculating the water, the simulated rainwater more closely reflected the real conditions of the city of León, without removing the elements typical of the industrial activity of this city. Although composition could vary from batch to batch, there were no reproducibility or repeatability issues with regard to the rainfall effect on the dolostone samples. The compositional characterization of the collected urban rainwater is presented for informative purposes in the Supporting Information (Table S1, Figures S2–S4, Supporting Information). Those analyses enabled to conclude that León is not currently exposed to the threat of acid rain.

Rainfall-Induced Erosion: Given the crucial importance of the temporal and spatial distribution of rainfall on the samples, a custom rain simulator was designed, fabricated, and calibrated.[39] It consisted of a metal structure, pipes, and sprinklers, with an approximate surface area of 4 m^2, and it was installed at a height of 10.5 m. The amount of artificial rainwater falling onto the samples aimed to reproduce a life cycle of 20 years (i.e., the average rainfall that any stone on the cathedral of León would be expected to withstand within a period of 20 years). The characteristics of the rainfall produced by the simulator replicated those of the annual accumulated precipitation in the city of León. More details in this regard can be consulted in ref. [39].

For the period of September 2020 through May 2021, the sample specimens were placed outdoors for exposure to natural temperature variations, and were subjected to 74 rainfall events totaling 545.8 mm of rain per hour, taking into account that each hour of simulated rainfall was equivalent to the mean accumulated rainfall in the city of León in a year.

Table 1. Set of thermal stress experiments applied to the dolostone samples.

2020	2020–2021 (Outdoors)	2021 (Moistened)
22 cycles $\Delta t = 34$ °C	310 days $\Delta t_{Max.} = 21.7$ °C $\Delta t_{Mean} = 10.8$ °C	2 cycles $\Delta t = 34$ °C

Thermal Erosion: A warm environment was recreated by placing the samples between two 1100 W electric heating plates (Trotec model TIH 1100 S), each with a surface temperature of 90 °C.[25] In addition, an auxiliary 250 W infrared heating lamp was also focused on the samples (**Figure 3**, left). As a result, a temperature of 30 °C was achieved on the surface of the samples, equivalent to the temperature experienced on an average summer day in the city of León. The temperature was measured using a Fluke model 566 Infrared Thermometer.[40]

To recreate a cold environment, the samples were homogeneously moistened with deionized water and placed in a JOCEL model JCH-300 chest freezer, with a 300 L capacity and a power of 45 kW h^{-1}, for 60 min. Inside the freezer chamber, a stable temperature of −18 °C was achieved, and the surface temperature of the samples reached −4 °C after one test cycle. This temperature was reached at night during the winter months in the city of León.[28,29] The samples were exposed to three types of temperature variations: artificially induced, drastic temperature variation, natural temperature variation (exposition outdoors), and temperature variations while the surface of the stones was wet.

For two months (January and February 2020), the stones were exposed to the thermal stress produced by hot and cold environments, interspersed with simulated rainfall cycles. In total, 22 temperature variation cycles were performed in the laboratory on each group of samples. The final thermal stress tests performed on the samples were preceded by a moistening of their surface before freezing in order to simulate the effects of frost when there is a high level of humidity present in a cold environment after rain. The entire set of temperature variations to which the stone samples were subjected are shown in **Table 1**. The samples were

divided into two groups to properly alternate between thermal stress and rainfall experiments. However, they were balanced to ensure that all the samples had the same minutes of rain and exposure to temperature variation.

2.4. Digitization for Determination of Wear in Stone Samples with a Structured-Light 3D Scanner

To determine the material loss in stone samples caused by the simulated climate-induced erosion, each dolostone specimen (both GO-coated and uncoated) was digitized three-dimensionally before and after the simulations. This was performed by a 3D scanner using structured light. The surface of each sample was measured by a Breuckmann smart SCAN^{3D}-HE scanner. This basically consisted of three parts: two 4-Mpx cameras, a blue light projector, and the support next to the field of view (FOV). Operation was via the emission by a projector of a structured light, a projection of a known light pattern, which was contrasted with the information captured by the two side cameras. According to the information received, the geometric shape of the studied object was triangulated. The accuracy of this type of scanner depended on the FOV, but its functional accuracy was estimated to be 9 μm for the samples in the present study.[41,42] OptoCAT software was used to manage the 3D scanning process.

Prior to measuring, the scanner was calibrated using a marker plate, whose exact dimensions were known, as a reference. The data obtained by the scanner cameras were subsequently compared to that obtained by the software. The scanner was positioned at a distance of 37 mm with a FOV of 125 mm. A series of projections were made on the table used to orient the sample, thus enabling the axis of rotation to be calculated and the position of the sample to be located on the table. The number of position changes of the sample relative to the scanner (in order to cover the whole surface) was determined. Given the geometry of the specimens, it was estimated that all the points on the surface could be obtained with four 90° turns. The intensity of the brightness exposure was graduated, and the most suitable exposure changes were chosen depending on the material, color, and texture of the object to be studied.[42] In each of the four scanning positions of a sample, the scanner performed four brightness exposures with different intensities depending on the capture range (shutter). Once all the captures were made, they were aligned and joined into a single 3D model. The model was exported in STL (stereolithography) file format, including only the created meshes representing the 3D shape, but not the surface image or color. The models in STL format of the sample before and after the erosion tests were imported into the "Geomatic Control" tool for comparison. The models were aligned, and the distance between homologous points of both was studied. In this way, it was possible to observe the loss of material caused by the erosion process. The deviations observed were of the order of 4 μm. It is important to clarify that a low standard deviation meant that a large number of the points with deviation were located at a specific distance. In contrast, a high standard deviation indicated that there have been significant deviations of the points in a more extensive range of values. During post-processing, the models were cleaned of possible interferences that may have been captured.

2.5. Properties of Dolostones after Applying the GO Coating

2.5.1. Determination of Color Changes with a Colorimetric Assay

A colorimetric test was performed to ascertain any color changes in the treated samples, both freshly coated and after the simulation tests. This followed the UNE-EN ISO/CIE 11664-4:2020 standard, also known as the CIELab method.[43] The parameters studied in this chromatic space were luminosity from black to white with the factor L^*, the amount of green-red with the factor a^*, and the amount of blue-yellow with the factor b^*, the latter two being the chromatic coordinates. The analysis began by calibrating the Konica Minolta model CR-5 colorimeter. Then, an aperture disc with a diameter of 8 mm was selected, through which three different measurements of each specimen were taken. In this way, the average stood as a more representative color determination of the surface of each. The difference, if any, in the three aforesaid parameters before and after a given situation would provide essential information on possible color changes experienced by the stones after GO coating and exposure to climate simulations. Additionally, analysis was made of the color difference ($\Delta E_{ab}{}^*$) between GO-coated and uncoated stones by calculating the Euclidean distance between the points representing them in the color space, following Equation (1). In general terms, the difference between the displayed color and the original color standard of the input content was quantified by $\Delta E_{ab}{}^*$. Lower $\Delta E_{ab}{}^*$ figures indicated greater accuracy, while high $\Delta E_{ab}{}^*$ levels indicated a significant mismatch.

$$\Delta E^*_{ab} = \sqrt{(\Delta L^*)^2 + (\Delta a^*)^2 + (\Delta b^*)^2}$$

The effect of the GO coating on the stone surface properties was further characterized using another two complementary techniques: diffuse reflectance UV–vis spectroscopy, in order to investigate the impact on the gloss and blackness, and contact angle measurements, to evaluate any effect on its surface hydrophilicity. The former was carried out using a Shimadzu UV-2401PC spectrophotometer, equipped with and integrating sphere, and using $BaSO_4$ as a white reference. The latter was carried out using the sessile drop method on a OneAttension Theta tensiometer, equipped with a CCD camera, and deionized water as the liquid droplet at room temperature.

2.5.2. Compression Test

An Ibertest press (Autotest 200/10 model) was used to perform compressive strength tests. A strain gauge load cell was used with a maximum compression capacity of 200 kN. From the pool of dolostone samples, 49 specimens were selected from the three different situations, namely uncoated specimens, and the two different GO coating surface concentrations (6.6 and 9.9 μg cm^{-2}, respectively) for testing. All specimens were compressed to a maximum strength of 200 kN, whether full breakage or not was achieved.

2.6. Endurance of the GO Coating Attached to the Dolostone Surface

In order to assess whether the GO coating was able to withstand the entire climate simulation procedure, two different qualitative aspects were analyzed: the composition of the rainwater leachates, and the surface of the stones before and after the GO coating and the climate simulations by means of microscopic observations.

2.6.1. Determination of Test Leachate Composition

Analysis was performed on the rainwater collected after physical contact with the surface of the GO-coated stone samples to ascertain the robustness of the coating and to detect any GO leakage into the surrounding environment. In a typical water sampling, 500 mL of simulated rainwater was collected from a homogenized pool after passing over 9 dolostones in each experimental situation (i.e., uncoated, and GO-coated with 6.6 or 9.9 μg cm^{-2} respectively). In addition, for comparative purposes, a fourth water sample was made up by dispersing 10 μg L^{-1} of GO in simulated rainwater (the equivalent to a theoretical full detachment from those samples with the highest amount of GO coating). This adulterated sample served as a benchmark against which to check the reliability of the tests. To avoid contaminating the collected water, glass trays previously washed with deionized water were used for auxiliary containment. The two techniques detailed below were applied to these water samples to determine the presence or not of GO, as well as the presence of other possible chemical species.

ICP-OES: The device used was a Xpectroblue-EOP-TI FMT26 (Spectro) spectrophotometer from Ametek that was capable of determining the atomic content of most of the elements in the periodic table. It could detect large concentrations that were quantifiable even in ppm. As per the ICP-OES determination, two measurements were taken for each sample, from which the average value was taken.

X-ray diffraction (XRD) was utilized to study the freeze-dried solid residue of the simulated rainwater samples. This was performed according to the Rietveld method with the EVA and TOPAS software (Bruker) and according to the UNE-EN 13925 (1-2-3) Standard[44] by means of a Bruker D8 Advance polycrystalline powder X-ray diffractometer, equipped with a Cu tube as the X-ray source (λ Cu Kα = 1.54 Å), with a tube voltage of 40 kV and a current of 40 mA. The results were recorded in Bragg–Brentano geometry in the range of $2\theta = (10–70°)$, with steps of 0.05° and 3 s accumulation time.

2.6.2. Microscopy Observations

The samples were subjected to microscopic visualization to gain insights into existing pores, microcrack propagation, and surface roughness. A JEOL 6100 LV scanning electron microscope equipped with an energy-dispersive spectrometer was used. Analyses were performed at a working distance of 10 mm, accelerating voltage of 20 kV, spot size of 50 μm, and current of 15 nA. The samples were not surface-sputtered with any conductive material prior to observation.

3. Results and Discussion

The climate simulations applied to the stone samples were devised to replicate the weathering that would be experienced during a period of 20 years in the city of León (Spain), which is home to a historical cathedral built from the same dolostone used as feedstock. After subjecting the sample specimens to the previously described erosive situations, the results of their characterization are described and discussed in the following.

3.1. Structured-Light 3D Scanner

The point clouds obtained from scanning the samples were compared both before and after the climate erosion tests to determine any deviations between both models. On average, these were made up of 1.5 million points with spatial position data at micrometric scale. Most of the disintegration suffered by the dolostone material was produced by its dissolution in water, denoted by a loss of material, that is, a negative deviation from the model. This type of deterioration facilitated deposition of the dissolved material inside other pores or small irregularities in the rough surface of the stone, which represented a positive deviation from the model. According to the color scale chosen to represent these data (**Figure 4**), the more reddish and yellowish tones represent this gain. In contrast, the actual material loss is identified by the more bluish tones. The most worn areas are the edges and corners, given that they are highly exposed due to their location.

This study is mainly focused on unraveling the extent of material loss. A certain amount of material separated from the bulk structure of the stones and was deposited at lower levels. The control samples analyzed (Figure 4a,b) had a higher mean deposition and loss than the treated samples. The standard deviations indicate the dispersion of the position variations when comparing the point clouds before and after the erosion tests.

It can be seen how both the average deposition and the average loss are higher in the uncoated samples, while the values for the groups of samples with 6.6 and 9.9 μg cm^{-2} surface GO concentrations are less marked in comparison with (and similar to) each other (Figure 4c,d,e,f). Similarly, the average standard deviations of the point clouds are higher in the control samples and have similar values to those of the two GO-coated samples. The normal distribution is Gaussian-like and represents the dispersion of values according to the standard deviation from the mean. In this way, some reference values are established to estimate the frequency of data repetition. The material loss data collected from the set of samples with the 9.9 μg cm^{-2} surface GO concentration have the lowest standard deviation values, indicating the least data scattering. Samples with a 6.6 μg cm^{-2} surface GO concentration have the same mean (Figures 4c–f,**5**). Since the standard deviation is more significant, as seen in the normal distribution (**Figure 5**), the dispersion of the data is more significant. With a higher mean of material loss and a standard deviation of 0.0029 mm, the set of uncoated samples have their standard distribution curve shifted to more negative values when compared to the other two (Figure 5). As indicated by the standard distribution theory, 64.2% of the values are within the standard distribution of the data. The dispersion of the data is low enough to confirm that these could be considered statistically reliable data, that is, a negligible variation in material loss with respect to the

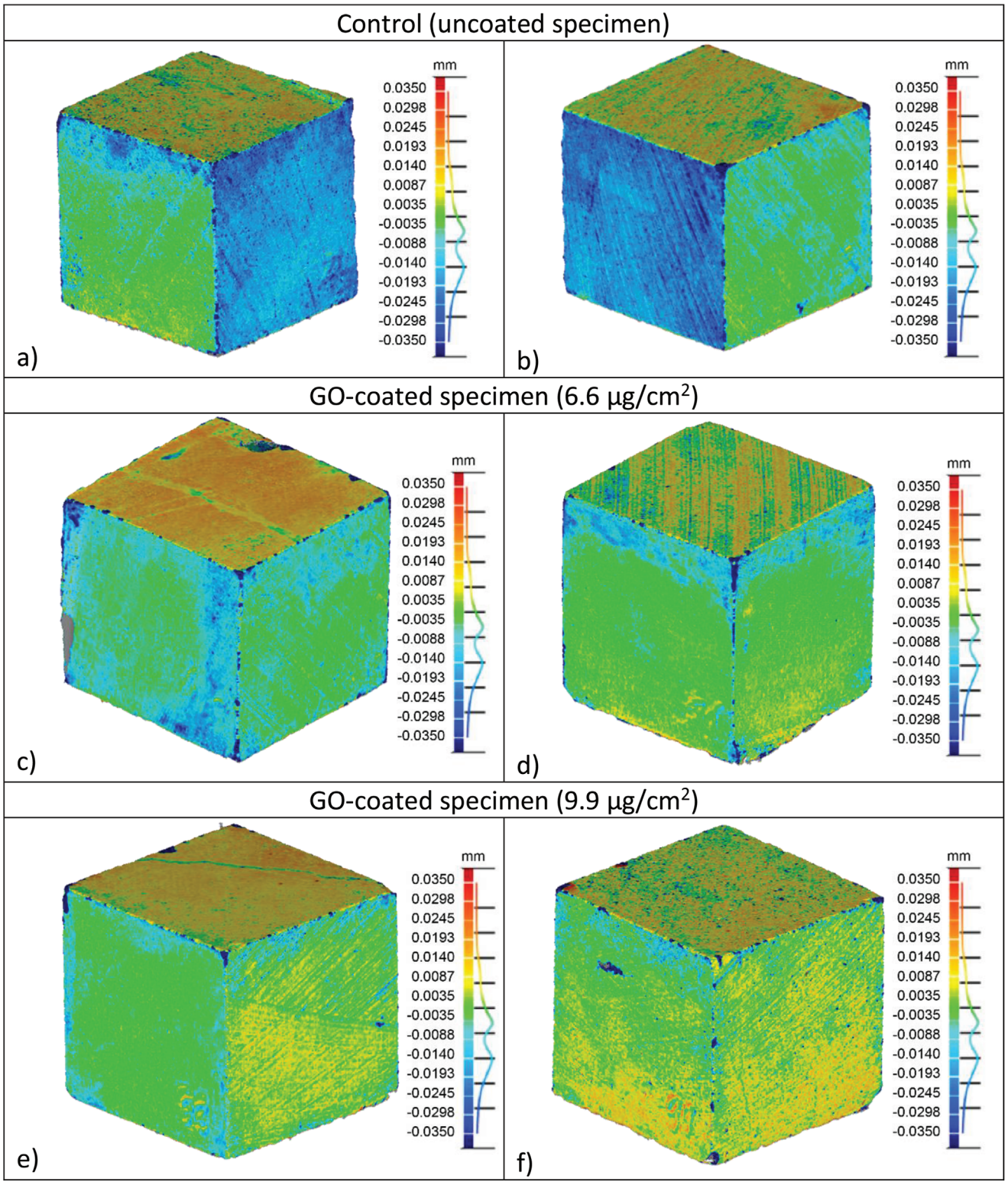

Figure 4. Different views of the 3D comparison of selected sample specimens created from the deviations between the point clouds before and after the erosion tests: a,b) Control sample; the rest are GO-coated with surface concentrations of c,d) 6.6 µg cm^{-2} and e,f) 9.9 µg cm^{-2}. All the cubes were exposed to simulated rainfall in their position in these views. Note that the bluest areas correspond to those undergoing the most erosion.

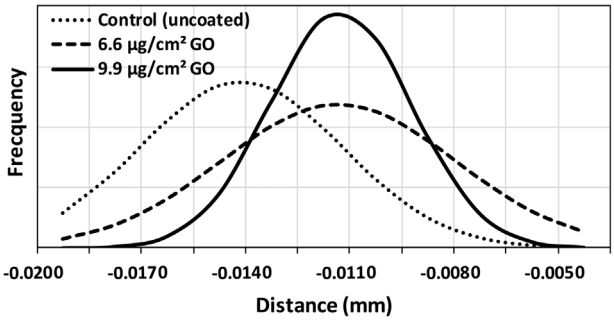

Figure 5. Representation of the normal distribution of the data collected from the 3D structured-light scanner digitization for each group of samples (coated and uncoated).

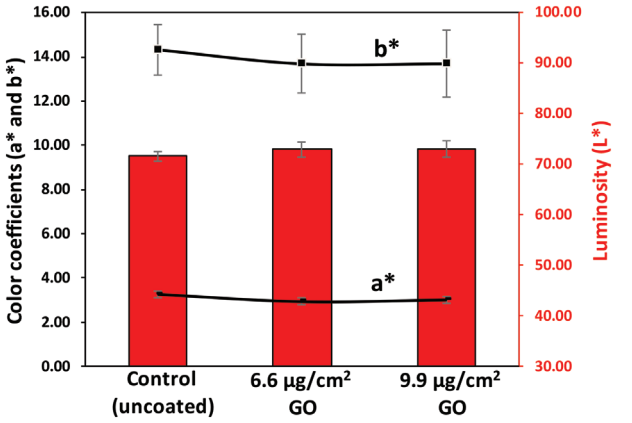

Figure 6. Representation of the average color coordinates and luminosity on the studied samples.

mean. Thus, the uncoated samples have a higher absolute deviation than the rest of the samples, which means they were eroded more than the GO-coated ones. The mean loss of material of the control set is −0.0149 mm, while the sets of samples with 6.6 and 9.9 µg cm^{-2} surface GO concentrations have a similar mean loss with a value of −0.0121 mm and −0.0120 mm, respectively, but with a narrower distribution in the latter case, indicative of an even lower degree of degradation. This indicates that the samples coated with GO show approximately up to 20% less material loss than the uncoated samples after the erosion tests carried out under simulated climate conditions equivalent to 20 years of rain in the city of León. In summary, we note that these results are analogous to those obtained by a photogrammetric technique and after being subjected to less intense climate simulation routines,[25] further evidencing the excellent protective effect of GO, beyond the initial studies.

3.2. Colorimetric Analysis

As stated earlier, preserving the aesthetics of monuments is a mandatory prerequisite to validate the application of a protective coating over their constituent materials. This implies negligible changes in color, brightness, or texture after applying the coating and over time. One of the aims of this work was to monitor for any possible color variation on the stone samples caused by the GO coating, given our preceding results,[25] where we ascertained a visible darkening of dolostones (therefore unviable for keeping the artistic value of the stone heritage intact) after exceeding a surface GO concentration of 10 µg cm^{-2}. It was theorized that the darkening that occurred after the excessive surface application of GO was due to a spontaneous partial reduction of GO at ambient conditions.[25]

Possible color variations were initially monitored by visual inspection throughout the process, and no color differences between the samples in each set could be inferred by the naked eye. More accurate colorimetric measurements were subsequently taken. An average of the variables collected in the triple data collection of the uppermost face of the cubic samples was taken, and the variation between the chromatic coordinates a^* and b^*, as well as in the luminosity L^*[43] was analyzed, for which the average values recorded are presented in **Figure 6**. As evidenced by these results, the color differences between each set of samples are compatible with being negligible to the naked eye. The color variations that occur naturally in each set cover a wider range than the application of GO as a coating could produce over time. However, the results of this colorimetric test suggest that any darkening did not occur outside of tolerable levels, and any that did were comparable to the natural color system (NCS) measurements previously reported.[25]

Table 2. Table of variations in the CIELAB color space factors of the samples studied.

	Control (uncoated)	6.6 µg cm^{-2} GO	9.9 µg cm^{-2} GO
L^*	71.51	72.91	73.01
ΔL^*	—	1.39	1.49
a^*	3.25	2.94	3.01
Δa^*	—	0.32	0.24
b^*	14.32	13.69	13.70
Δb^*	—	0.63	0.63
ΔE_{ab}^*	—	1.56	1.64

The average colorimetric data of the samples in each set is summarized in **Table 2**, as well as the differences between the three types of stimuli compared to the control samples. In terms of color variation (Δa^*, Δb^*, and ΔE_{ab}^*), both GO-coated samples display negligible differences with respect to the uncoated stone, and they are not dependent on the amount of applied GO within this range. More specifically, such low ΔE_{ab}^* values are not noticeable to the naked eye.

According to the results obtained, it can be concluded that GO did not affect the natural color of the samples either by darkening or by changes in tonality. This means that GO does not alter the chromatic properties of the samples within the range of the applied surface concentrations (i.e., not more than 10 µg cm^{-2}).

As shown previously, a spontaneous partial reduction process enables GO to darken the stone surfaces on which it is applied as a coating.[25] However, the results of the colorimetric test indicate that this darkening does not acquire any significance, given the low amounts deposited on the surface. Thus it may be concluded that the proposed tolerable blackness threshold of 7% (with respect to the uncoated counterparts)[25] was not exceeded. Moreover, the coated samples have a slightly more luminous color, as judged by a marginally higher L^* for the higher surface

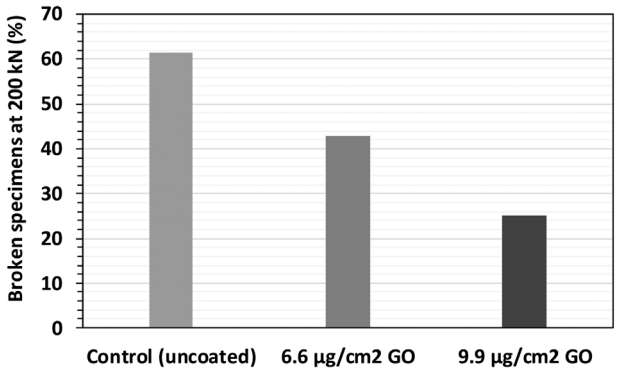

Figure 7. Ratio of dolostone specimens that underwent breakage at the maximum stress applied during the compression test (200 kN).

concentration of GO. Nevertheless, this difference is imperceptible to the human eye, and its variability lies more within the typical color varieties of limestone and dolomite.

Additional characterization by diffuse reflectance UV–vis spectroscopy (Figure S5, Supporting Information) and contact angle measurements (Figure S6, Supporting Information), over both uncoated and GO-coated stone samples confirmed the above results. The GO protective coating (in the surface concentration range herein reported) does not induce any change on the aesthetics or gloss, while keeping the native hydrophilicity of the base material.

3.3. Compression Tests

One of the most harmful events that a dolostone can experience is mechanical failure due to the infiltration of water within its bulk structure. Such water uptake may lead to partial dissolution and gelifraction phenomena, causing internal cracks and voids that eventually deplete their mechanical and structural performance, sometimes drastically.[45] Hence, as previously explained, an effective coating material should (among other properties) prevent the infiltration of water during a precipitation event, justifying our mechanical monitoring of the stone specimens after climate simulations (**Figure 7**). Given the high intrinsic hardness of Boñar dolostone, not all of them experienced full breakage after reaching the maximum load applied (200 kN). This fact was of practical use to determine the extent to which these stones experienced or not full breakage at such stress. It was observed that 38.5% of the uncoated control specimens had a compressive strength higher than 200 kN. In the specimens with a 6.6 µg cm^{-2} surface GO concentration, the proportion whose endurance exceeded 200 kN increased to 57%, finally reaching 75% in the specimens with a 9.9 µg cm^{-2} surface GO concentration. These are very significant results as they clearly show how the GO coating is able to preserve the mechanical resistance of the dolostones, even after experiencing very intense climate simulations.

3.4. Leachate Analysis

One of the most critical aspects in developing a coating to protect exposed surfaces is that it must be as harmless as possible for both the surrounding substrate material and the environment.[46] After intense downpours pass over the surface of stones and the water subsequently drains away, there is a risk that the nanomaterials in the coating could leach into the surroundings, posing health and/or environmental hazards. For this reason, a thorough analysis of these water leachates was performed by ICP-OES, specifically targeting Al, Ca, Mg, and Si as the most plausible ion sources contained in the studied dolostones. The obtained results are given in **Figure 8**. For comparative purposes, and in order to highlight the magnitude difference in ionic content, some average or range values from Spanish municipal water systems and commercial bottled waters, respectively, are also shown.

In addition to the ICP-OES determination, the existence of measurable amounts of organic carbon, that is, compounds with carbon–carbon bonds, was explored. Accordingly, total organic carbon (TOC) tests were performed to roughly estimate the presence of organic carbon (a common interference in ICP-OES determination), with values in the 6–10 mg L^{-1} range. For this reason, it was decided to further check the validity of the analyses by analytical displacement, that is, adding known amounts (1 and 5 mg L^{-1}) of each of the targeted elements to a selected sample (leachate from uncoated stones), prior to repeating the ICP-OES determination. This strategy eventually verified that the encountered amounts of dissolved organic carbon did not distort the formation of the plasma, and therefore did not affect the measurements. In general terms, such a scarce presence of organic carbon hinted at a low or null presence of GO in the leachates. For all the studied leachates, it was determined that Al and Si levels were below the detection limit (0.05 mg L^{-1} in solution). The average amount of Ca in the 97 leading Spanish bottled water brands, as well as the average Ca contained in 50 municipal water systems in Spain[47,48] offered perspective on the normal concentrations of these elements in drinking water (i.e., much higher than those found in the leachates). It can be deduced that the leaching of dolostone components by the action of the rainfall simulations was practically nonexistent, with no notable differences between the different protection treatments.

The solid fraction contained in the leachates was isolated by freeze-drying. The obtained powder was analyzed by XRD and Raman spectroscopy (data not shown), and no trace of GO was found by either of these techniques, in contrast to the adulterated water sample, which clearly showed the presence of GO. By combining both the ICP-OES determination of the leachates and the characterization of their solid residues, it can be reasonably concluded that GO did not detach from the stone or leached out in any way during the climate simulations. This is in line with our previous observations[25] from which we postulated plausible mechanisms for these phenomena. However, further studies will be needed in order to fully unravel the origins of such a strong bond between GO and the dolostone surface.

3.5. SEM Analysis

SEM was used to characterize the surface of the stones (fresh untested, and those undergoing climate simulations), and to identify possible changes to their surface morphology after the tests (**Figure 9**). The four dolostone types showed a similar

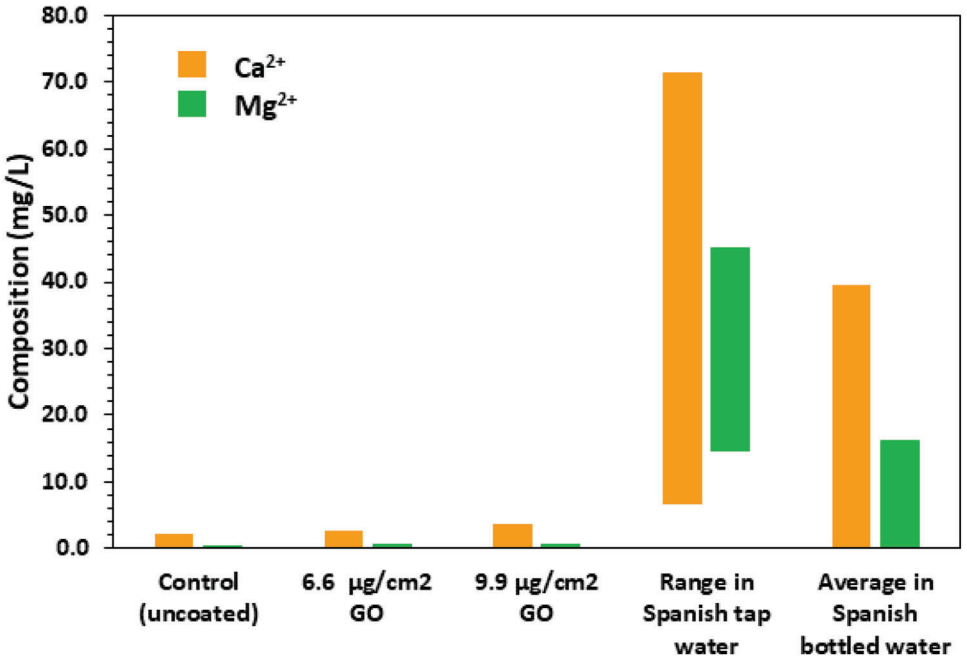

Figure 8. Results of the ICP-OES analyses on the collected simulated rainwater after the experiments. Note that no Al^{3+} or Si^{4+} values are given as those cations did not exceed the detection limit (<0.05 mg L^{-1}). The data regarding calcium[47] and magnesium[48] for Spanish municipal water systems were obtained from sources in the literature.

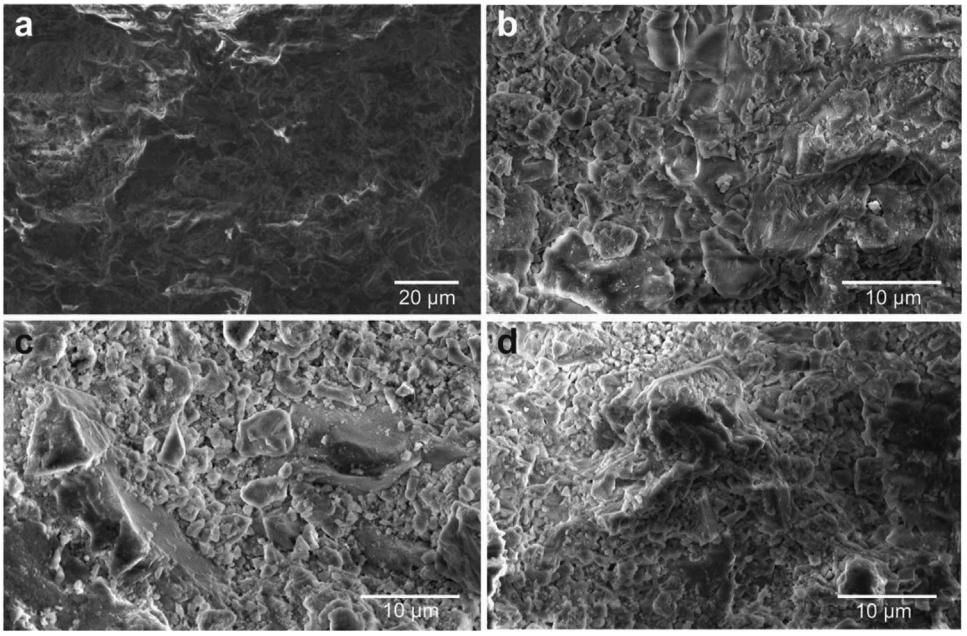

Figure 9. SEM images of the surface of dolostones. a) Fresh untested stone, and tested stones by climate simulation: b) uncoated, c) 6.6 µg cm^{-2} GO, d) 9.9 µg cm^{-2} GO.

surface profile. However, as seen in Figure 9b, the uncoated sample seems to show a higher surface roughness and a more quartered aspect than the fresh and untreated dolostone (Figure 9a), likely due to the effect of climate simulation. While this increased roughness and quartering is similar to those of the sample coated with a 6.6 µg cm^{-2} surface GO concentration, the optimum coating (set as 9.9 µg cm^{-2} GO) shows a more regular roughness that is much more similar to the fresh stone. This suggests that the improvement could be noticed even at a microscopic level, but this is only a qualitative support to the 3D scanning of the surface of the stones, which clearly evidenced this effect at a higher resolution.

4. Conclusions

The present research has made it possible to reaffirm the results obtained in the previous work[25] and represents a step forward toward implementing GO as a protective coating for monumental dolostone. The main conclusions drawn are summarized as follows:

- The results obtained by structured-light 3D scanner indicate that the stones coated with GO experience up to ≈20% less of material loss compared to the control samples after climate simulations equivalent to 20 years of rain and temperature in a model northern Spanish city.
- The data evidence that GO adheres firmly to dolostone and makes it resistant to disintegration in an aqueous environment.
- The optimal surface concentration of GO is 9.9 μg cm^{-2} without causing color differences after application of the coating, even after a year elapsed, so it is aesthetically and optically innocuous. In this way, the stones acquired a highly protective barrier against natural erosive agents without significant changes to their visual aesthetics.
- After studying the solid residue of the water collected from the rainfall tests, no presence (not even the slightest trace) of GO was detected, reinforcing the premise that it binds very strongly to the stone and implying that this treatment is environmentally-safe and does not produce any polluting leachate.

In summary, this research further proves and highlights the extraordinary properties of GO for use as a monumental/ornamental stone coating. It opens up a wide range of possibilities in terms of protection and durability, not only for stone but for other types of building materials exposed to inclement weather, such as ceramic, concrete and mortar, and/or other stone-based materials. Furthermore, with the advancement of research in this field, it is estimated that GO coatings could acquire other beneficial properties, such as UV protection and resistance to freeze–thaw processes, carbonation, acid rain, etc. Overall, GO has great potential as a protective coating for stones: it is affordable, easy to apply, it has high theoretical durability in the very long term, and the results achieved so far support the premise of being the ultimate, or at least one of the best solutions for the conservation and protection of monuments without altering their artistic and cultural values. In future studies, attempts of simulated erosion on the samples for the equivalent of more extended periods of time, such as 50 years, will be pursued, in order to challenge the durability and protection limits of the GO coating.

Supporting Information

Supporting Information is available from the Wiley Online Library or from the author.

Acknowledgements

This research received funding from the University of León (ULE-PoC 2018) and Fundación General de la ULE y de la Empresa (FGULEM) under projects 2019/00149/001 and 2020. This research was also funded through an awarded MICINN project (PID2020-120439RA-I00). The authors are also thankful to the "Applied innovation against climate change and other aggressions on stone monuments (PRESERVARTE)" project of the Regional Ministry of Culture and Tourism of Castilla y León, which will be used to complement this research in the future.

Conflict of Interest

The authors declare no conflict of interest.

Author Contributions

Conceptualization: J.M.G.-D., M.F.-R., R.M.-G.; Investigation: R.M.-G., D.G.-C., F.J.F.-F., A.O.-M, A.M.C., P.C., S.G.; Writing—Original: R.M.-G., D.G.-C., F.Z.; Draft Preparation: A.O.-M, P.C., S.G., F.J.F.-F., F.Z. J. M. G.-D.; Writing—Review & Editing: P.C., R.M.-G., J. M. G.-D.; Supervision: J.M.G.-D., M.F.-R., R.M.-G.; Funding: J.M.G.-D., M.F.-R. All authors have read and agreed to the published version of the manuscript.

Data Availability Statement

The data that support the findings of this study are available from the corresponding author upon reasonable request.

Keywords

coatings, dolostone, durability, erosion, graphene oxide, heritages, limestone

Received: March 28, 2023
Revised: May 2, 2023
Published online:

[1] L. Carcavilla, J. Durán Valsero, Á. García-Cortés, J. López-Martínez, *Geoheritage* **2009**, *1*, 75.
[2] BOE.es – BOE-A-1985-12534 Ley 16/1985, de 25 de Junio, Del Patrimonio Histórico Español. https://www.boe.es/buscar/act.php?id=BOE-A-1985-12534 (accessed: January 2023).
[3] F. Choay, *Main trends of research in the social and human sciences*, Volume 1, Pages 818 –842, https://doi.org/10.1515/9783111532394-032.
[4] Centre,U.W.H. Centro del Patrimonio Mundial. https://whc.unesco.org/es/list/ (accessed: January 2023).
[5] N. C. Leitão, D. B. Lorente, *Energies* **2020**, *13*, 4838.
[6] J. Khinast, G. F. Krammer, Ch. Brunner, G. Staudinger, *Chem. Eng. Sci.* **1996**, *51*, 623.
[7] M. Lion, F. Skoczylas, B. Ledésert, *Int. J. Rock Mech. Mining Sci.* **2005**, *42*, 508.
[8] M. Gomez-Heras, S. McCabe, *Coastal Fluxes Anthropocene* **2015**, *11*, 1.
[9] C. J. de Madariaga, *J. Cult. Heritage Manage. Sustainable Dev.* **2021**, *11*, 614.
[10] M. C. V. Calvo, S. Martínez-Ramírez, M. A. de Buergo, R. F. González, *Spectrosc. Lett.* **2012**, *45*, 146.
[11] G. A. Pope, T. C. Meierding, T. R. Paradise, *Geomorphology* **2002**, *47*, 211.
[12] P. Brimblecombe, *J. Inst. Conserv.* **2014**, *37*, 85.
[13] C. Sabbioni, P. Brimblecombe, R.-A. Lefèvre, *Pollut. Atmos.* **2009**, *203*, 157.

[14] S. Basu, S. A. Orr, Y. D. Aktas, *Atmosphere* **2020**, *11*, 788.
[15] F. Oduber, A. I. Calvo, A. Castro, C. Blanco-Alegre, C. Alves, G. Calzolai, S. Nava, F. Lucarelli, T. Nunes, J. Barata, R. Fraile, *Sci. Total Environ.* **2021**, *754*, 142045.
[16] A. Luque, G. Cultrone, E. Sebastián, O. Cazalla, *Mater. Constr. (Madrid, Spain)* **2008**, *58*, 115.
[17] H. A. Viles, N. Cutler, *Global Change Biol.* **2012**, *18*, 2406.
[18] UNESCO Centro Del Patrimonio Mundial – Available online: https://whc.unesco.org/es/list/ (accessed: July 2022).
[19] P. Baglioni, D. Chelazzi, R. Giorgi, *Nanotechnologies in the Conservation of Cultural Heritage* **2015**, 15–59, https://doi.org/10.1007/978-94-017-9303-2_2.
[20] P. Nanocoat *26/2005 Art.21. L'impiego Di Nanotecnologie e Nanomateriali per Il Recupero e La Conservazione Dei BeniCulturali*, **2005**;
[21] R. Archeomatica : https://www.archeomatica.it/eventi/convegno-nuove-tecnologie-per-il-recupero-e-la-conservazione-dei-beni-culturali (accessed: January 2023).
[22] M. M. Alrashed, M. D. Soucek, S. C. Jana, *Prog. Org. Coat.* **2019**, *134*, 197.
[23] B. Healy, T. Yu, D. Da, S. Alves, C. B. Breslin, *Corros. Mater. Degrad.* **2020**, *1*, 296.
[24] M. J. Nine, M. A. Cole, D. N. H. Tran, D. Losic, *J. Mater. Chem. A* **2015**, *3*, 12580.
[25] D. González-Campelo, M. Fernández-Raga, Á. Gómez-Gutiérrez, M. I. Guerra-Romero, J. M. González-Domínguez, *Adv. Mater. Interfaces* **2021**, *8*, 2101012.
[26] A. Antolín-Rodríguez, D. Merino-Maldonado, Á. Rodríguez-González, M. Fernández-Raga, J.-M. González-Domínguez, A. Juan-Valdés, J. García-González Statistical Study of the Effectiveness of Surface Application of Graphene Oxide as a Coating for Concrete Protection, submitted.
[27] A. Antolín-Rodríguez, D. Merino-Maldonado, A. Juan-Valdés, J.-M. González-Domínguez, M. Fernández-Raga, J. García-González Performance of Graphene Oxide as a Coating Nanomaterial for Improving the Surface Characteristics of Concrete Structures, submitted.
[28] C. Blanco-Alegre, A. Castro, A. I. Calvo, F. Oduber, E. Alonso-Blanco, D. Fernández-González, R. M. Valencia-Barrera, A. M. Vega-Maray, R. Fraile, *Q. J. R. Meteorol. Soc.* **2018**, *144*, 2715.
[29] A. E. de Meteorología Valores climatológicos normales – Agencia Estatal de Meteorología – AEMET. Gobierno de España Available online: https://www.aemet.es/es/serviciosclimaticos/datosclimatologicos/valoresclimatologicos (accessed: January 2023).
[30] D. Dollimore, J. G. Dunn, Y. F. Lee, B. M. Penrod, *Thermochim. Acta* **1994**, *237*, 125
[31] C. S. Hurlbut, C. Klein *Manual of Mineralogy*, Wiley, New York **1985**.
[32] M. Agudo, A. U. de los, *Arqueol. Territ. Medieval* **2017**, *24*, 185.
[33] P. Vázquez, F. J. Alonso, L. Carrizo, E. Molina, G. Cultrone, M. Blanco, I. Zamora, *Constr. Build. Mater.* **2013**, *41*, 868.
[34] DIN EN 1926:2007-03 Natural Stone Test Methods – Determination. https://tienda.aenor.com/norma-din-en-1926-2007-03-95610059 (accessed: January **2023**).
[35] DIN EN 15801:2010-04 Conservation of Cultural Property – Test. https://tienda.aenor.com/norma-din-en-15801-2010-04-119869065 (accessed: January 2023).
[36] W. S. Hummers, R. E. Offeman, *J. Am. Chem. Soc.* **1958**, *80*, 1339.
[37] D. C. Marcano, D. V. Kosynkin, J. M. Berlin, A. Sinitskii, Z. Sun, A. Slesarev, L. B. Alemany, W. Lu, J. M. Tour, *ACS Nano* **2010**, *4*, 4806.
[38] M. Fernandez-Raga, A. Castro, E. Marcos, C. Palencia, R. Fraile, *Int. J. Climatol.* **2017**, *37*, 1834.
[39] M. Fernández-Raga, I. Rodríguez, P. Caldevilla, G. Búrdalo, A. Ortiz, R. Martínez-García, *Water* **2022**, *14*, 3831.
[40] Home | Fluke Process Instruments, https://www.flukeprocessinstruments.com/en-us (accessed: January 2023).
[41] S. Giganto, P. Zapico, M. Á. Castro-Sastre, S. Martínez-Pellitero, P. Leo, P. Perulli, *Procedia Manuf.* **2019**, *41*, 698.
[42] S. Martínez-Pellitero, E. Cuesta, S. Giganto, J. Barreiro, *Opt. Lasers Eng.* **2018**, *110*, 193.
[43] UNE-EN ISO 11664-4:2011 Colorimetría. Parte 4: Espacio Cromático L*a*b* CIE 1976. (ISO 11664-4:2008). *Aenor: Madrid, España* **2008**.
[44] UNE-EN 13925-1:2006 Ensayos No Destructivos. Difracción de Rayos X Aplicada a Materiales Policristalinos y Amorfos Parte 1: Principios Generales. *Aenor: Madrid, España* **2006**.
[45] V. Rives, J. Garcia-Talegon, *Mater. Sci. Forum* **2006**, *514–516*, 1689.
[46] A. Artesani, F. Di Turo, M. Zucchelli, A. Traviglia, *Coatings* **2020**, *10*, 217.
[47] I. Vitoria, F. Maraver, C. Ferreira-Pêgo, F. Armijo, L. M. Aznar, J. Salas-Salvadó, *Nutr. Hosp.* **2014**, *30*, 188.
[48] F. Maraver, I. Vitoria, C. Ferreira-Pêgo, F. Armijo, J. Salas-Salvadó, *Nutr. Hosp.* **2015**, *31*, 2297.